

Highly Effective Removal of Methylene Blue Using a Chemi-Mechanical Pretreated Cellulose-based Superabsorbent Hydrogel

Yan Lin,^{a,b,*} Guigan Fang,^{a,b,*} Yongjun Deng,^{a,b} Kuizhong Shen,^{a,b} Ting Wu,^{a,b} and Man Li^{a,b}

Eucalyptus bleached chemical pulp was fibrillated using a PFI pulp beater and ball mill method and was modified by acryloyl chloride. A novel porous cellulose-based hydrogel was prepared from the modified cellulose and acrylic acid for the removal of methylene blue (MB) from aqueous solution. The structure and morphology of the hydrogel were characterized by Fourier transform infrared spectroscopy (FT-IR) and scanning electron microscopy (SEM), respectively. The influence of various parameters, such as pH value, hydrogel dosage, initial MB concentration, and contact time on the dye adsorption, were investigated. The equilibrium experimental data fitted well to the Langmuir isotherm model, and the maximum adsorption capacity of the hydrogel reached 3003 mg/g. In addition, the reusability study suggested that the hydrogel showed great adsorption capacity and a high removal ratio, even after the 5th adsorption-desorption cycle. Thus, the modified cellulose-based hydrogel is a potential superabsorbent for the removal of MB from wastewater.

Keywords: Cellulose; Superabsorbent hydrogel; Adsorption; Methylene blue

Contact information: a: Institute of Chemical Industry of Forestry Products, CAF; Key Lab. of Biomass Energy and Material, Jiangsu Province; National Engineering Lab. for Biomass Chemical Utilization; Key and Open Lab. on Forest Chemical Engineering, SFA, Nanjing 210042, PR China; b: Collaborative Innovation Center for High Efficient Processing and Utilization of Forestry Resources, Nanjing Forestry University, Nanjing 210037, PR China; *Corresponding authors: linyan@icifp.cn; fanguigan@icifp.cn

INTRODUCTION

Organic dyes, which are widely used in various fields such as textiles, paper, plastics, and cosmetics, are the main contributor to colored effluents (Ravikumar *et al.* 2005). It is estimated that over 100,000 commercial dyes weighing over 700,000 tons are produced every year, and about 10 to 20% of that weight is discharged in effluent from manufacturing processes or application industries (Piccin *et al.* 2012). Some organic dyes cause allergic diseases and skin irritation, while others are carcinogenic and highly toxic, thus causing serious environmental problems and endangering human health (Rafatullah *et al.* 2010). Therefore, it is crucial to remove hazardous materials from effluent.

Due to the high hydrophilicity and stability to light or heat of dyes, many technologies have been used to treat colored wastewater (Wang *et al.* 2013; Cai *et al.* 2015; Tran *et al.* 2017). Adsorption is one of the most favorable techniques for removing dyes (Nghah *et al.* 2011; Popa and Visa 2017; Khoshnevis *et al.* 2018). Polysaccharide-based absorbents are gaining attention because of their renewable, biodegradation, and non-toxic behavior (Sun *et al.* 2015; Góes *et al.* 2016; Xu *et al.* 2018).

Cellulose, the most abundant polysaccharide on earth, is widely used as the raw material for hydrogel absorbents to remove dyes and heavy metals from effluent (Xiong *et*

al. 2014). Cellulose-based hydrogels are commonly formed by three-dimensional cross-linked polymer networks, which absorb and retain water and solute molecules. In wastewater treatment, modified cellulose-based hydrogels exhibit excellent adsorption properties. Dai and Huang (2016) reported that modified pineapple peel cellulose hydrogels embedded with sepia ink exhibited a high removal of methylene blue (MB). Liu *et al.* (2015) prepared a cellulose-based bioadsorbent that effectively removes anionic and cationic dyes. Wang *et al.* (2017b) prepared a novel polyacrylic acid-grafted quaternized cellulose adsorbent with a high adsorption capacity for MB at 1735 mg/g. Many hydrogels based on cellulose derivatives (Wang *et al.* 2010; Chen *et al.* 2017; Salama 2018) and composite cellulose-based hydrogels (Peng *et al.* 2016; Yang *et al.* 2016) have been studied. Thus, novel cellulose-based hydrogels are a topic of interest for researchers and are expected to replace the traditional adsorbents in the future.

In this study, a novel porous cellulose-based hydrogel was prepared for wastewater treatment. After PFI beating and ball mill processes, eucalyptus bleached chemical pulp powder was modified with acryloyl chloride and grafted with acrylic acid by free radical polymerization. The cellulose-based hydrogel was characterized using Fourier transform infrared spectroscopy (FT-IR) and scanning electron microscopy (SEM). MB was taken as the study model, the adsorption behavior characterized by kinetics and isotherm analysis, and the reuse of the prepared hydrogel were investigated. Based on the results, the chemi-mechanical pretreatment and the modification of the pulp were very effective method to enhance the adsorption of cellulose-based hydrogel, which has potential to be used in environmental applications. Besides, the study provides theoretical basis for exploring the high value-added utilization of wood pulp.

EXPERIMENTAL

Materials

Commercial eucalyptus bleached chemical pulp (α -cellulose > 90%) was purchased from Hainan Jinhai Pulp and Paper Co., Ltd. (Hainan, China). The average length of the fiber (L_w) was 0.626 μm , and the average width was 15.8 μm . MB was in the form of an analytically pure grade and purchased from the Tianjin Institute of Chemical Reagents (Tianjin, China). All other reagents were analytical grade and used without further purification. Distilled water was used for dissolution, polymerization reactions, swelling, and adsorption studies.

Synthesis of porous modified cellulose-based hydrogels

The eucalyptus bleached chemical pulp was first fibrillated using a PFI pulp beater (IMT, Dongguan, China) and planetary ball mill. The pulp was torn (30 g, oven dry) into pieces, defibrillated, and filtered at 25 °C. The filter cake (10%, wt) as treated by a PFI beater (12000 r) and dried in a vacuum at 40 °C. The dry pulp was ball-milled at 360 rpm for 72 h. The machine worked for 1 h and rested for 0.5 h, repeatedly. The obtained eucalyptus pulp powder in the valve bag was stored in a dryer at 25 °C for 24 h.

The dry pulp powder (1.6 g) was immersed in 250 mL of acetonitrile at 30 °C for 1 h. Potassium tert-butoxide (3.37 g) in acetonitrile was added and stirred at 30 °C for 4 h. Acryloyl chloride (5.43 g) in acetonitrile was added slowly. The reaction was stirred at reflux for 24 h and then filtered. The product was washed with water and ethanol and dried at 40 °C under a vacuum (Trombino *et al.* 2009) to obtain the light yellow acryloyl

cellulose.

A solution of NaOH/urea/H₂O (weight ratio of 7:12:81) was cooled to -12 °C. The acryloyl cellulose (0.083 g) was added and stirred vigorously for 30 min until the solution was transparent (Luo and Zhang 2009). After the cellulose solution was heated to 60 °C for 0.5 h, ammonium persulfate solution, acrylic acid, and methylene-bis-acrylamide solution were added. The reaction continued at this temperature until the hydrogel was obtained. After the reaction, the hydrogel was separated, washed with distilled water, and cut into small pieces. These hydrogel pieces were immersed in distilled water for 48 h to remove the unreacted chemicals. The distilled water was refreshed every 6 h. After the pieces were freeze-dried for 72 h, the porous cellulose-based hydrogel was obtained.

Characterization

FT-IR spectra of the eucalyptus pulp powder, acryloyl cellulose, and dry hydrogel were taken on a Nicolet iS10 Model FT-IR Spectrometer (Thermo Electron, Waltham, MA, USA) in the range of 4000 to 500 cm⁻¹. The morphology of the hydrogel was observed by SEM on a Hitachi S-3400N (Tokyo, Japan).

The swelling study

The swelling property of the prepared hydrogel was studied (Sun *et al.* 2013; Bhattacharyya and Ray 2015). The dried hydrogel sample was immersed in distilled water at 25 °C for 72 h. The swollen sample was taken out in specific time intervals, dried with filter water, and weighed. The weight of the hydrogel was measured three times until the weight was constant and the average result was calculated. The swelling ratio (S_t) of the hydrogel sample was calculated using Eq. 1,

$$S_t = (W_t - W_0)/W_0 \quad (1)$$

where W_0 is the initial weight of dry hydrogel (g) and W_t is the weight of swollen hydrogel at time (g).

Measurements of the dye adsorption

The adsorption property of the cellulose-based hydrogel for cationic dye removal of MB was studied in this work (Mohammed *et al.* 2015; Kumari *et al.* 2016). The dry hydrogel samples were each immersed in 50 mL MB solutions and placed in a constant shaking incubator at 25 °C at a speed of 100 rpm. For adsorption kinetics, 50 mg dried hydrogel samples were immersed in 100 mL MB solution with concentration of 200 mg/L or 1000 mg/L and placed in a constant shaking incubator at 25 °C at a speed of 100 rpm. At the specific time intervals, the hydrogels were separated, and the concentration of the MB solutions after adsorption was determined at $\lambda_{\max} = 664$ nm with a UV spectrophotometer (T6 New Century, Beijing, China). The effects of the pH value, the hydrogel dosage, contact time, and initial MB concentration on the dye adsorption were evaluated. The adsorption capacity of MB (q_t , mg/g) at different time intervals (t) was calculated by Eq. 2. The removal ratio of MB (R) was determined using Eq. 3,

$$q_t = (C_0 - C_t)V/m \quad (2)$$

$$R = (C_0 - C_t)/C_0 * 100\% \quad (3)$$

where C_0 and C_t are the concentration of the MB solution at the initial time and at time t , respectively (mg/L), V is the volume of the MB solution (mL), and m is the mass of the dry hydrogel sample (g).

Reusability of the cellulose-based hydrogel

A dry modified cellulose-based hydrogel sample (20 mg) was added into 50 mL of the MB solution (200 mg/L, pH = 7). After 6 h, the hydrogel containing MB was separated and desorbed in 30 mL HCl solution (0.1 M) three times. Then, the hydrogel sample was washed with distilled water three times and used for the next cycle. The above adsorption-desorption experiments were repeated five times and the concentration of the MB solution after the adsorption was determined with a UV spectrophotometer. Then, the adsorption capacity and removal of MB for each cycle were calculated using the above equations.

RESULTS AND DISCUSSION

Preparation and FT-IR Characterization of the Hydrogel

The supermolecular structure of cellulose is formed by partial crystallization, and the domains of dense crystal structure of cellulose hinder reactions and applications. The crystal areas of pulp fiber can be destroyed after PFI grinding, and the crystallization of the pulp fiber can decline rapidly in the ball mill (Schwanninger *et al.* 2004; Xu *et al.* 2013). In this paper, eucalyptus bleached chemical pulp was pretreated with a PFI beater and ball mill to enhance the reactivity of cellulose. The pretreated pulp powder was used as raw material to prepare cellulose-based hydrogels *via* esterification and polymerization with acrylic acid.

Figure 1 illustrates the FT-IR spectra of (a) pretreated eucalyptus cellulose powder, (b) acryloyl cellulose, and (c) cellulose-based hydrogel. Figure 1b shows that the modified acryloyl cellulose generally kept its original structure feature of cellulose powder. The absorbance at 1727 cm^{-1} was ascribed to C=O stretching, which confirmed the presence of the modified cellulose with acrylate groups. In Fig. 1c, the very wide and strong absorbance at 2500 to 3700 cm^{-1} was attributed to the hydrogen bonded between the OH groups and COOH groups in the network. The absorbance at 1700 cm^{-1} can be attributed to the overlap effects of the C=O stretching bands of the carbonyl groups from the modified cellulose, acrylic acid, and methylene-bis-acrylamide (Guilherme *et al.* 2005; Paulino *et al.* 2006). In addition, the absorption bands at 1556 cm^{-1} and 1402 cm^{-1} in Fig. 1c were likely due to asymmetric stretching vibration and symmetric stretching vibration of COO^- .

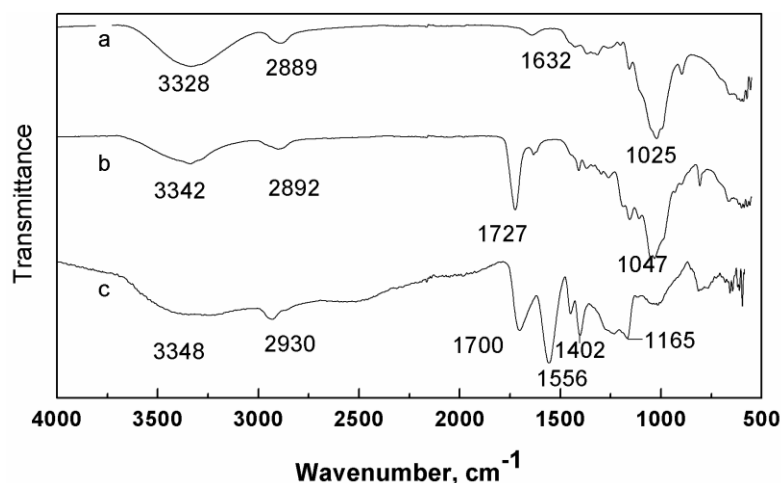


Fig. 1. FT-IR spectra of (a) pretreated eucalyptus cellulose powder, (b) acryloyl cellulose, and (c) cellulose-based hydrogel

Morphology Analysis

The photograph and SEM micrograph of the freeze-dried hydrogel is illustrated in Fig. 2. In Fig. 2a, grooves and uniform pores were observed in and out of the dry hydrogel, which were also shown in the SEM micrograph. Figure 2b confirmed the three-dimensional network structure of the prepared hydrogel. The porous structure allowed for the spread of water and dye molecules into the hydrogel and enhanced the swelling and dye adsorption property of the hydrogel.

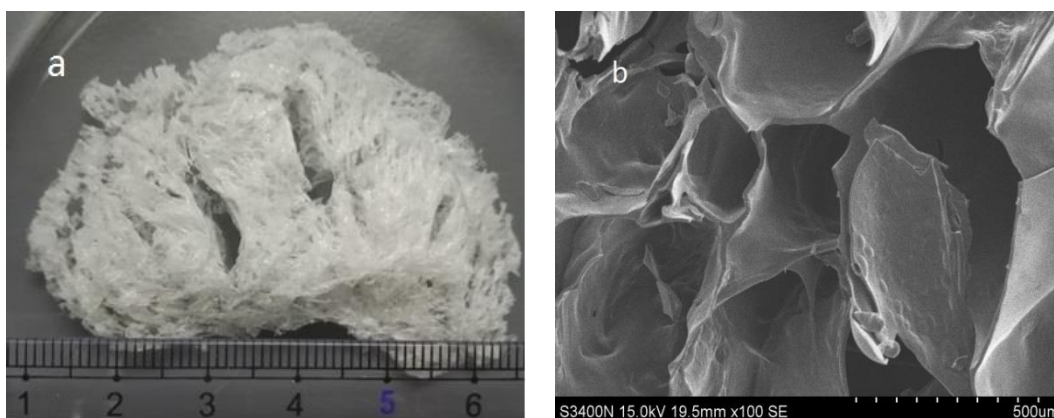


Fig. 2. Photograph and SEM micrograph of cellulose-based hydrogel

Swelling Property of the Hydrogel

Several cellulose-based hydrogels were prepared by varying the mass ratio of acrylic acid to modified cellulose. The equilibrium swelling ratio of the hydrogels is shown in Fig. 3a. The equilibrium swelling ratio of the hydrogels increased first, then decreased and reached a maximum at 888 g/g when the mass ratio was 10:1 (Gel-2). This result suggests that more acrylic acid grafted onto the cellulose chains was helpful for the swelling. However, excess acrylic acid was more likely liable to self-polymerize rather than graft onto the hydrogel network, so the swelling property of the hydrogel degraded. The dynamic swelling behavior of Gel-2 was studied, as shown in Fig. 3b. The swelling ratio increased with time and reached equilibrium at about 72 h. Because Gel-2 showed the highest equilibrium swelling ratio, it was chosen for the following adsorption studies.

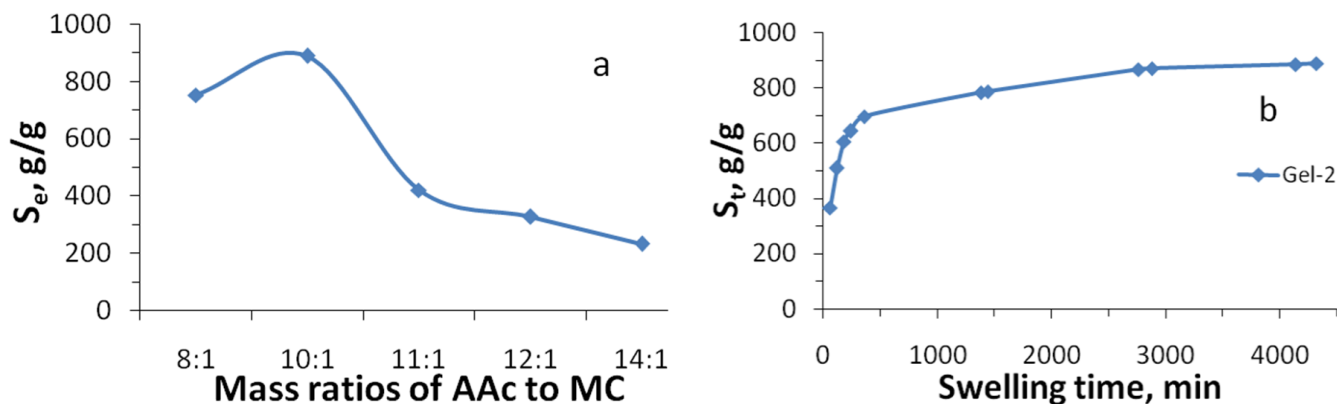


Fig. 3. Effect of mass ratios of acrylic acid and modified cellulose on swelling ratio (a), swelling curve of the cellulose-based hydrogel (b)

Effect of pH on the Adsorption Property

The cellulose-based hydrogel was pH-sensitive due to the COOH and COO⁻ groups in the polymer. The effect of pH on the MB removal is shown in Fig. 4. The removal of MB increased significantly from 30.8 to 92.4% when the pH was changed from 2 to 4. The color removal increased very slowly until it reached a maximum of 97.9% at pH 7 and then, decreased gradually at pH > 7. This phenomenon was attributed to the interactions between MB molecules and the hydrogel network and the swelling property of the hydrogel. MB exhibited a positive charge in aqueous solutions. The COO⁻ and COOH groups in the hydrogel would convert with each other in different pH conditions. In the solution of pH=2, the ionization of COOH was inhibited, and the COO⁻ groups converted to COOH, which was unfavorable to the combination with MB molecules. Meanwhile, the hydrogen bonding effect between the COOH groups and OH groups strengthened at this situation, leading to shrinkage of the hydrogel network and hindering diffusion and adsorption of the dye. Therefore, the removal ratio was not high in pH 2 solution. As the pH value increased, the COOH groups in the hydrogel ionized and the hydrogel network expanded, resulting in increased dye removal. Particularly, there was a sharp increase of the color removal at pH 4. It can be inferred the *pKa* of the hydrogel was approximately pH 4, as reported previously for a superabsorbent hydrogel made of modified polysaccharide (Paulino *et al.* 2006). At pH 11, the cellulose chain hydrolyzed, leading to decreased dye adsorption. Therefore, the prepared hydrogel showed a great MB adsorption at pH 4 to 10 and best at pH 7.

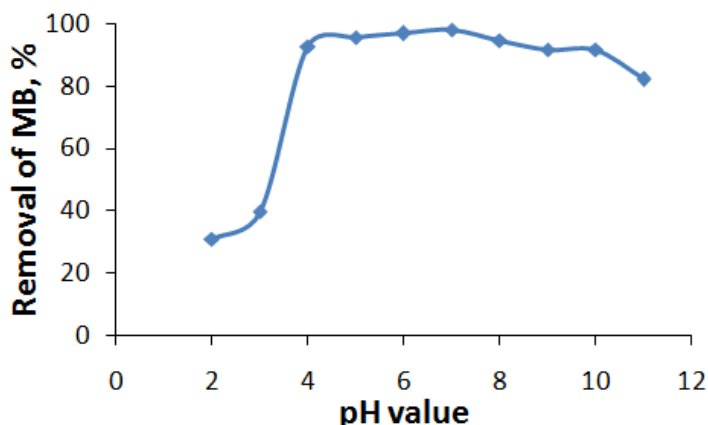


Fig. 4. Effect of pH value on the dye adsorption

Effect of the Hydrogel Dosage on the Adsorption Property

Figure 5 represented the effect of different hydrogel dosages on the adsorption of MB. The experiments were conducted in 50 mL of a 200 mg/L MB solution at pH 7 for 6 h. The results showed that the removal ratio was more than 90% for different dosages of hydrogel, and it increased as the hydrogel dosage increased, though it was less in the last two tests. This result suggested that the cellulose-based hydrogel had a great adsorption effect on MB. In the dye solution with higher hydrogel dosage (80 mg and 100mg), the removal ratio decreased a little compared with that in solution with 50 mg hydrogel. This was because that higher dosage of hydrogel can absorb more water, resulting in a higher concentration of MB remaining in the solution. Though the removal ratio obtained by 50 mg hydrogel was a little higher than that at 20 mg, a further adsorption study was carried out for the 20 mg hydrogel sample for economic reasons.

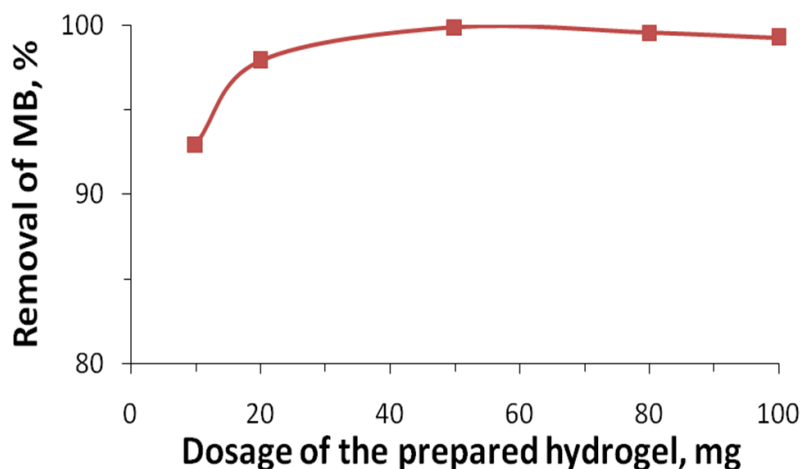


Fig. 5. Effect of the hydrogel dosage on the dye adsorption

Effect of Contact Time on the Adsorption Property

The effect of contact time on the adsorption of MB by the hydrogel was studied. The results are illustrated in Fig. 6. As shown, a similar trend of the adsorption capacity curve and removal ratio curve was observed under different concentrations of MB. These trends increased significantly at first, then increased slowly and tended to reach equilibrium with the increase of contact time. At the beginning of the adsorption process, the active banding sites on the hydrogel were unoccupied and available for the MB molecules, resulting in a rapid increase of adsorption capacity. As the time continued, the banding sites were occupied gradually; thus the adsorption rate rose slowly and reached dynamic equilibrium with a maximum adsorption value (Bhattacharyya and Ray 2013). The results indicated that the equilibrium adsorption capacity of the dye was 995 mg/g in the 200 mg/L MB solution and 2712 mg/g in the 1000 mg/L solution, respectively.

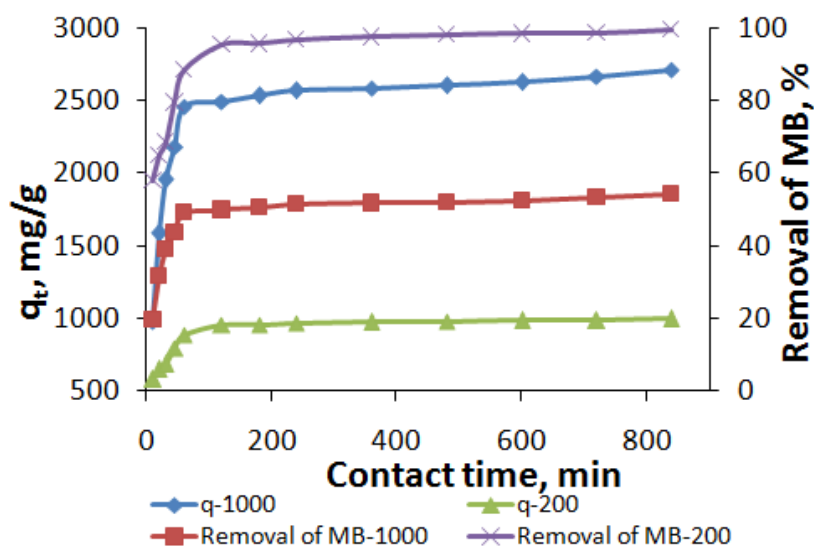


Fig. 6. Effect of contact time on the dye adsorption

To investigate the potential rate-controlled process involved in the adsorption, the adsorption kinetics were evaluated by the pseudo 1st order (Eq. 4), pseudo 2nd order (Eq. 5) (Li *et al.* 2014), and the intraparticle diffusion model (Eq. 6) (Mahmoodi 2011),

$$\lg(q_e - q_t) = \lg q_e - \frac{k_1 t}{2.303} \quad (4)$$

$$\frac{t}{q_t} = \frac{1}{k_2 q_e^2} + \frac{t}{q_e} \quad (5)$$

$$q_t = k_i t^{0.5} + C \quad (6)$$

where q_e and q_t (mg/g) are the adsorption amounts at equilibrium and at time t , respectively, k_1 (min⁻¹) and k_2 (g·mg⁻¹·min⁻¹) are the rate constants of the pseudo 1st order and pseudo 2nd order kinetic models, respectively, k_i is the intraparticle diffusion rate constant (mg·g⁻¹·min^{-0.5}), and C is a constant related to the thickness of the boundary layer.

Table 1. Adsorption Kinetic Parameters of the Modified Cellulose-Based Hydrogel

C ₀ , mg/L	q _{exp} ^a , mg/g	Pseudo 1 st Order Model			Pseudo 2 nd Order Model		
		k ₁ ×10 ⁻³ , min ⁻¹	q _e , mg/g	R ²	k ₂ ×10 ⁻⁵ , g·mg ⁻¹ ·min ⁻¹	q _e , mg/g	R ²
200	994.85	4.606	248.89	0.777	10.149	1003.01	0.999
1000	2711.99	2.303	788.86	0.724	2.676	2717.39	0.999

^a Experimental data.

The related kinetic parameters of the pseudo 1st order and pseudo 2nd order kinetic models are listed in Table 1. The R² of the pseudo 2nd order kinetic model was much higher than that of the pseudo 1st order kinetic model and the calculated q_e by the pseudo 2nd order kinetic model in two MB solutions were very close to the experimental value. It indicated that the adsorption process of MB by the hydrogel followed the pseudo 2nd order kinetic model.

Because the transport of MB molecules in the solution was involved in the adsorption, the adsorption was investigated using the intraparticle diffusion model (Eq. 3c). The parameters of this model are listed in Table 2. It was clear that the adsorption process occurred in two stages, and the adsorption rate was controlled by the first stage for $k_{i,1} > k_{i,2}$. In the first stage, the MB molecules diffused and were adsorbed onto the external surface of the hydrogel. When the adsorption sites on the exterior surface were saturated, the MB molecules diffused into the interior of the hydrogel and then were adsorbed in the second stage. The intercept $C > 0$ in Table 2 suggested that intraparticle diffusion is not the only rate limiting step (Ely *et al.* 2009). Besides, the rather low R² values in Table 2 indicated a relatively poor fit to the model, suggesting that the interparticle diffusion is not the only mechanism.

Table 2. Parameters of Intraparticle Diffusion Model

C ₀ (mg/L)	k _{i,1} (mg·g ⁻¹ ·min ^{-0.5})	k _{i,2} (mg·g ⁻¹ ·min ^{-0.5})	k _i (mg·g ⁻¹ ·min ^{-0.5})	Intercept C (mg/g)	R ²
200	65.79	3.86	13.48	679.7	0.672
1000	312.5	10.86	43.11	1674	0.569

Effect of Initial Dye Concentration on the Adsorption

The effect of the initial MB concentrations on the adsorption property of the hydrogel was studied. The results are shown in Fig. 7. Notably, the adsorption capacity increased almost linearly when the initial dye concentration ranged from 300 mg/L to 1200 mg/L. Then, it slowly increased to 2927 mg/g. In contrast, the removal ratio of MB decreased with the increased initial concentration. It could be ascribed to the limited adsorption sites on the hydrogel. Once the active sites were saturated, the adsorption capacity tended to the equilibrium, while the removal ratio decreased significantly owing to the excess dye molecules.

To evaluate the adsorption mechanism, the adsorption isotherm of MB by the hydrogel was fitted by the Langmuir isotherm (Eq. 7) and Freundlich isotherm (Eq. 8) (Zhang *et al.* 2014). A dimensionless constant separation factor, R_L , seen in Eq. 9, reflects whether the adsorption was favorable or unfavorable (Wang *et al.* 2017a).

$$\frac{C_e}{q_e} = \frac{C_e}{q_m} + \frac{1}{q_m b} \quad (7)$$

$$\ln q_e = \frac{1}{n} \ln C_e + \ln K_f \quad (8)$$

$$R_L = \frac{1}{1+bC_0} \quad (9)$$

where q_m is the maximum adsorption capacity (mg/g), C_e is the equilibrium concentration of the MB solution (mg/L), b is the Langmuir adsorption equilibrium constant (L/mg), K_f is the Freundlich constant, and parameter n is related to the adsorption capacity. The greater the n value is, the better the adsorption performance. Generally, it is considered that the adsorption occurs easily when the n value ranges from 2 to 10 and the adsorption happens difficultly when $n < 0.5$.

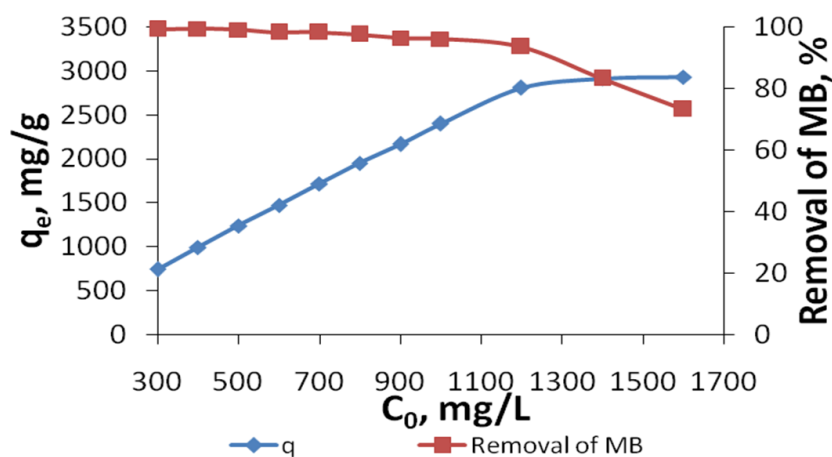


Fig. 7. Effect of the initial concentration of MB on the dye adsorption

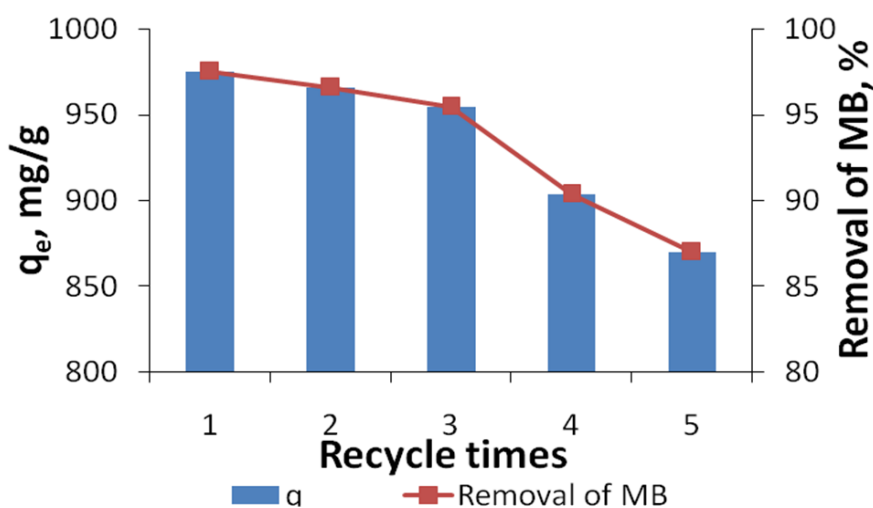
Table 3. Adsorption Isotherm Parameters of the Prepared Hydrogel

Langmuir model			Freundlich model		
q_m (mg/g)	B (L/mg)	R^2	K_f	n	R^2
3003.00	0.11	0.999	786.82	3.89	0.872

Table 4. The q_m Values for the Adsorption of MB on Different Adsorbents

Adsorbents	q_m (mg/g)	Ref.
Modified cellulose-based hydrogel	3003	Present work
Cellulose-based bioadsorbent	1372	(Liu <i>et al.</i> 2015)
Cellulose nanocrystal-alginate hydrogel beads	256.41	(Mohammed <i>et al.</i> 2015)
Cellulose nanocrystals	118 to 769	(Batmaz <i>et al.</i> 2014)
Cellulose-graft-acrylic acid hydrogels	2197	(Zhou <i>et al.</i> 2011)
Cellulose nanowhiskers-based polyurethane foam	554.8	(Kumari <i>et al.</i> 2016)
Activated carbon	980.3	(Rafatullah <i>et al.</i> 2010)

The parameters of two models are listed in Table 3. The coefficient of determination for the Langmuir model ($R^2=0.999$) was much closer to unity and much larger than that of the Freundlich model. This suggested that the Langmuir isotherm was more appropriate to describe the adsorption process demonstrated by the hydrogel and the monolayer adsorption of MB occurred on the surface of the hydrogel. Moreover, the calculated q_m of the hydrogel was 3003 mg/g. Table 4 shows that the modified cellulose-based hydrogel showed much higher q_m than the cellulose-based adsorbents and over three times q_m than the activated carbon. This testified the outstanding adsorption property of MB by the prepared hydrogel. It was speculated that the prominent adsorption by the hydrogel had a relationship with the pretreatment of the cellulose raw material by the PFI beater and ball mill (Schwanninger *et al.* 2004; Xu *et al.* 2013). According to Eq. 9 and $b = 0.11$ in Table 3, it was obvious that the separation factor (R_L) value was less than 1 under various initial concentration conditions, which implied favorable adsorption of the process (Wang *et al.* 2017a). In addition, the coefficient $n = 3.89$ in the Freundlich isotherm was larger than 2, which indicated that the MB was easily adsorbed onto the prepared hydrogel. Thus, the modified cellulose-based hydrogel can be effectively used as an adsorbent in the treatment of effluents containing MB.

**Fig. 8.** Reusability of the hydrogel for methylene blue adsorption

Reusability of the Hydrogel

The reusability of the prepared hydrogel is shown in Fig. 8. Interestingly, the hydrogel presented an excellent adsorption property of MB with the adsorption capacity of 955 mg/g and the removal ratio up to 95.5 %, even in the 3rd cycle. After that, the adsorption capacity and the removal ratio decreased to some extent in the next two cycles. This may be ascribed to the mass loss of the hydrogel in the experiments and the incomplete desorption of dye on the hydrogel during the desorption process. Even so, the removal ratio was 87.0 % with the adsorption capacity of 870 mg/g after five cycles. Thus, the prepared modified cellulose-based hydrogel could be a reusable alternative superabsorbent for the removal of MB.

CONCLUSIONS

1. A novel porous modified cellulose-based hydrogel was prepared by modified cellulose and acrylic acid after the pretreatment and modification of eucalyptus bleached chemical pulp. The structure and morphology of the hydrogel was characterized using FT-IR and SEM.
2. The maximum swelling ratio of the hydrogel was 888 g/g with the mass ratio of acrylic acid to modified cellulose as 10:1.
3. The hydrogel presented great adsorption of MB at a pH of 4 to 10. According to the Langmuir isotherm, the maximum adsorption capacity of the hydrogel equaled 3003 mg/g.
4. The prepared hydrogel can be regenerated and reused and the removal ratio of MB reached 87.0 % in the 5th cycle.

ACKNOWLEDGEMENTS

The work was supported by the Natural Science Foundation of Jiangsu Province of China (Grant number: BK20160151), the Research Grant of Jiangsu Province Biomass Energy and Materials Laboratory (Grant number: JSBEM-S-201510), and the 13th Five-Year the State Key Development Program (Grant number: 2017YFD0601005).

REFERENCES CITED

- Batmaz, R., Mohammed, N., Zaman, M., and Minhas, G. (2014). "Cellulose nanocrystals as promising adsorbents for the removal of cationic dyes," *Cellulose* 21(3), 1655-1665. DOI: 10.1007/s10570-014-0168-8
- Bhattacharyya, R., and Ray, S. K. (2013). "Kinetic and equilibrium modeling for adsorption of textile dyes in aqueous solutions by carboxymethyl cellulose/poly(acrylamide-co-hydroxyethylmethacrylate) semi-interpenetrating network Hydrogel," *Polymer Engineering and Science* 53(11), 2439-2453. DOI: 10.1002/pen.23501
- Bhattacharyya, R., and Ray, S. K. (2015). "Application of industrial dyes by semi-IPN

- hydrogels of acrylic copolymers and sodium alginate,” *Journal of Industrial and Engineering Chemistry* 22, 92-102. DOI: 20.1016/j.jiec.2014.06.029
- Cai, T., Li, H., Yang, R., and Li, A. (2015). “Efficient flocculation of an anionic dye from aqueous solutions using a cellulose-based flocculant,” *Cellulose* 22(2), 1439-1449. DOI: 10.1007/s10570-015-0571-9
- Chen, P., Liu X., Jin, R., and Nie, W. (2017). “Dye adsorption and photo-induced recycling of hydroxypropylcellulose/molybdenum disulfide composite hydrogels,” *Carbohydrate Polymers* 167, 36-43. DOI: 10.1016/j.carbpol.2017.02.094
- Dai, H., and Huang, H. (2016). “Modified pineapple peel cellulose hydrogels embedded with sepia ink for effective removal of methylene blue,” *Carbohydrate Polymers* 148, 1-10. DOI: 10.1016/j.carbpol.2016.04.040
- Ely, A., Baudu, M., Basly, J. P., and Kankou, M. O. S. A. O. (2009). “Copper and nitrophenol pollutants removal by Na-montmorillonite/alginate microcapsules,” *J. Hazard Mater.* 171(1-3), 405-409. DOI: 10.1016/j.jhazmat.2009.06.015
- Góes, M. M., Keller, M., Oliveira, V. M., and Villalobos, L. D. G. (2016). “Polyurethane foams synthesized from cellulose-based wastes: Kinetics studies of dye adsorption,” *Industrial Crops and Products* 85, 149-158. DOI: 10.1016/j.indcrop.2016.02.051
- Guilherme, M. R., Reis, A. V., Takahashi, S. H., and Rubira, A. F. (2005). “Synthesis of a novel superabsorbent hydrogel by copolymerization of acrylamide and cashew gum modified with glycidyl methacrylate,” *Carbohydrate Polymers* 61, 464-471. DOI: 10.1016/j.carbpol.2005.06.017
- Khoshnevis, H., Mint, S. M., Yedinak, E., Tran, T. Q., Zadhoush, A., Youssefi, M., Pasquali, M., and Duong, H. M. (2018). “Super high-rate fabrication of high-purity carbon nanotube aerogels from floating catalyst method for oil spill cleaning,” *Chemical Physics Letters* 693, 146-151. DOI: 10.1016/j.cplett.2018.01.001
- Kumari, S., Chauhan, G. S., and Ahn, J. H. (2016). “Novel cellulose nanowhiskers-based polyurethane foam for rapid and persistent removal of methylene blue from its aqueous solutions,” *Chemical Engineering Journal* 304, 728-736. DOI: 10.1016/j.cej.2016.07.008
- Li, L., Luo, C., Li, X., Duan, H., and Wang, X. (2014). “Preparation of magnetic ionic liquid/chitosan/graphene oxide composite and application for water treatment,” *International Journal of Biological Macromolecules* 66(5), 172-178. DOI: 10.1016/j.ijbiomac.2014.02.031
- Liu, L., Gao, Z. Y., Su, X. P., and Chen, X. (2015). “Adsorption removal of dyes from single and binary solutions using a cellulose-based bioadsorbent,” *ACS Sustainable Chemical Engineering* 3(3), 432-442. DOI: 10.1021/sc500848m
- Luo, X., and Zhang, L. (2009). “High effective adsorption of organic dyes on magnetic cellulose beads entrapping activated carbon,” *Journal of Hazardous Materials* 171(1-3), 340-347. DOI: 10.1016/j.jhazmat.2009.06.009
- Mahmoodi, N. M. (2011). “Equilibrium, kinetics, and thermodynamics of dye removal using alginate in binary systems,” *Journal of Chemical Engineering Data* 56(6):2802-2811. DOI: 10.1021/je101276x
- Mohammed, N., Grishkewich, N., Berry, R. M., and Tam, K.C. (2015). “Cellulose nanocrystal-alginate hydrogel beads as novel adsorbents for organic dyes in aqueous solutions,” *Cellulose* 22(6), 3725-3738. DOI: 10.1007/s10570-015-0747-3
- Ngah, W. S. W., Teong, L. C., and Hanafiah, M. A. K. M. (2011). “Adsorption of dyes and heavy metal ions by chitosan composites: A review,” *Carbohydrate Polymers* 83(4), 1446-1456. DOI: 10.1016/j.carbpol.2010.11.004

- Paulino, A. T., Guiherme, M. R., Reis, A.V., and Campese, G.M. (2006). "Removal of methylene blue dye from an aqueous media using superabsorbent hydrogel supported on modified polysaccharide," *Journal of Colloid and Interface Science* 301(1), 55-62. DOI: 10.1016/j.jcis.2006.04.036
- Peng, N., Hu, D., Zeng, J., Li, Y., Liang, L., and Chang, C. (2016). "Superabsorbent cellulose-clay nanocomposite hydrogels for highly efficient removal of dye in water," *ACS Chemistry and Engineering* 4(12), 7217-7224. DOI: 10.1021/acssuschemeng.6b02178
- Piccin, J. S., Gomes, C. S., Feris, L. A., and Gutterres, M. (2012). "Kinetics and isotherms of leather dye adsorption by tannery solid waste," *Chemical Engineering Journal* 183(8), 30-38. DOI: 10.1016/j.cej.2011.12.013
- Popa, N., and Visa, M. (2017). "The synthesis, activation and characterization of charcoal powder for the removal of methylene blue and cadmium from wastewater," *Advanced Powder Technology* 28(8), 1866-1876. DOI: 10.1016/j.appt.2017.04.014
- Rafatullah, M., Sulaiman, O., Hashim, R., and Ahmad, A. (2010). "Adsorption of methylene blue on low-cost adsorbents: A review," *Journal of Hazardous Materials* 177(1-3), 70-80. DOI: 10.1016/j.jhazmat.2009.12.047
- Ravikumar, K., Deebika, B., and Balu, K. (2005). "Decolourization of aqueous dye solutions by a novel adsorbent: Application of statistical design and surface plots for the optimization and regression analysis," *Journal of Hazardous Materials* 122(1), 75-83. DOI: 10.1016/j.jhazmat.2005.03.008
- Salama, A. (2018). "Preparation of CMC-g-P(SPMA) super adsorbent hydrogels: Exploring their capacity for MB removal from waste water," *International Journal of Biological Macromolecules* 106, 940-946. DOI: 10.1016/j.ijbiomac.2017.08.097
- Schwanninger, M., Rodrigues, J. C., Pereira, H., and Hinterstoisser, B. (2004). "Effects of short-time vibratory ball milling on the shape of FT-IR spectra of wood and cellulose," *Vibrational Spectroscopy* 36(1), 23-40. DOI: 10.1016/j.vibspec.2004.02.003
- Sun, X., Gan, Z., Jing, Z., and Wang, H. (2015). "Adsorption of methylene blue on hemicellulose-based stimuli-responsive porous hydrogel," *Journal of Applied Polymer Science* 132(10), 41606-41615. DOI: 10.1002/app.41606
- Sun, X., Wanf, H., Jing, Z., and Mohanathas, R. (2013). "Hemicellulose-based pH-sensitive and biodegradable hydrogel for controlled drug delivery," *Carbohydrate Polymers* 92, 1357-1366. DOI: 10.1016/j.carbpol.2012.10.032
- Tran, T. Q., Headrick, R. J., Bengio, E. A., Myo Myint S., Khoshnevis, H., Jamali, V., Duong, H. M., and Pasquali, M. (2017). "Purification and dissolution of carbon nanotube fibers spun from the floating catalyst method," *ACS Applied Materials & Interfaces* 42(9), 37112-37119. DOI: 10.1021/acsmi.7b09287
- Trombino, S., Cassano, R., Bloise, E., and Muzzalupo, R. (2009). "Synthesis and antioxidant activity evaluation of a novel cellulose hydrogel containing *trans*-ferulic acid," *Carbohydrate Polymers* 75(1), 184-187. DOI: 10.1016/j.carbpol.2008.05.018
- Wang, J., Wang, W., and Wang, A. (2010). "Synthesis, characterization and swelling behaviors of hydroxyethyl cellulose-g-poly(acrylic acid)/attapulgit superabsorbent composite," *Polymer Engineering and Science* 50(5), 1019-1027. DOI: 10.1002/pen.21500
- Wang, N., Jin, R. N., Omer, A. M., and Ouyang, X. K. (2017a). "Adsorption of Pb(II) from fish sauce using carboxylated cellulose nanocrystal: Isotherm, kinetics, and thermodynamic studies," *International Journal of Biological Macromolecules* 102,

- 232-240. DOI: 10.1016/j.ijbiomac.2017.03.150
- Wang, Q., Tian, S., Cun, J., and Ning, P. (2013). "Degradation of methylene blue using a heterogeneous Fenton process catalyzed by ferrocene," *Desalination and Water Treatment* 51(28-30), 5821-5830. DOI: 10.1080/19443994.2012.763047
- Wang, Y., Zhang, C., Zhao, L., and Meng, G. (2017b). "Cellulose-based porous adsorbents with high capacity for methylene blue adsorption from aqueous solutions," *Fiber and Polymers* 18(5), 891-899. DOI: 10.1007/S12221-017-6956-7
- Xiong, J., Jiao, C., Li, C., and Zhang, D. (2014). "A versatile amphiprotic cotton fiber for the removal of dyes and metal ions," *Cellulose* 21(4), 3073-3087. DOI: 10.1007/s10570-014-0318-z
- Xu, M., Xu, M., Dai, H., and Wang, S. (2013). "The effects of ball milling and PFI pretreatment on the cellulose structure and fiber morphology," *Journal of Cellulose Science and Technology* 21(2), 46-52.
- Xu, R., Mao, J., Peng, N., Luo, X., and Chang, C. (2018). "Chitin/clay microspheres with hierarchical architecture for highly efficient removal of organic dyes," *Carbohydrate Polymers* 188, 143-150. DOI: 10.1016/j.carbpol.2018.01.073
- Yang, H., Sheikhi, A., and van de Ven, T. G. (2016). "Reusable green aerogels from cross-linked hairy nanocrystalline cellulose and modified chitosan for dye removal," *Langmuir* 32(45), 11771-11779. DOI: 10.1021/acs.langmuir.6b03084
- Zhang, G., Yi, L., Deng, H., and Sun, P. (2014). "Dyes adsorption using a synthetic carboxymethyl cellulose-acrylic acid adsorbent," *Journal of Environmental Sciences* 26(5), 1203-1211. DOI: 10.1016/S1001-0742(13)60513-6
- Zhou, Y., Fu, S., Liu, H., and Yang, S. (2011). "Removal of methylene blue dyes from wastewater using cellulose-based superadsorbent hydrogels," *Polymer Engineering and Science* 51(12), 2417-2424. DOI: 10.1002/pen.22020

Article submitted: June 20, 2018; Peer review completed: July 18, 2018; Revised version received and accepted: September 26, 2018; Published: October 16, 2018.
DOI: 10.15376/biores.13.4.8709-8722